

Selective Photo-Oxygenation of Light Alkanes Using Iodine Oxides and Chloride

Nichole S. Liebov,^[a] Jonathan M. Goldberg,^[b] Nicholas C. Boaz,^[b, c] Nathan Coutard,^[a] Steven E. Kalman,^[a, d] Thompson Zhuang,^[b] John T. Groves,^{*[b]} and T. Brent Gunnoe^{*[a]}

Partial oxidation of light alkanes to generate alkyl esters has been achieved under photochemical conditions using mixtures of iodine oxides and chloride salts in trifluoroacetic acid (HTFA). The reactions are catalytic in chloride and are successful using compact fluorescent light, but higher yields are obtained using a mercury lamp. In this photo-initiated oxyesterification process, the robust alkyl ester products are resistant to over-oxidation, and under optimized conditions yields for alkyl ester production

of ~50% based on methane, ~60% based on ethane (with a total functionalized yield of EtX (X=TFA or Cl) of 80%) and ~30% based on propane have been demonstrated. The reaction also proceeds in aqueous HTFA and dichloroacetic acid with lower yields. Mechanistic studies indicate that the process likely operates by a chlorine hydrogen atom abstraction pathway wherein alkyl radicals are generated, trapped by iodine, and converted to alkyl trifluoroacetates *in situ*.

Introduction

Natural gas is an abundant fuel resource and chemical feedstock.^[1] Traditionally, light alkanes are converted to higher value chemicals by processes that require high temperature and pressure. For example, methane can be functionalized by initial steam reforming to generate synthesis gas (H₂/CO) and subsequently converted to methanol or long-chain hydrocarbons using Fischer-Tropsch chemistry.^[2] However, this process for the conversion of methane to liquid fuels and chemicals is capital- and energy-intensive.^[3] The ethane and propane components of natural gas are cracked at high temperatures (> 900 °C) to generate ethylene and propylene, respectively, which serve as precursors for a variety of higher value chemicals.^[4] The demand for efficient use of energy and the need for on-site conversion of natural gas to liquids have provided motivation to develop new methods for direct and selective low-temperature (< 200 °C) light alkane oxy-functionalization.^[5] But, a key

goal and major challenge is to develop processes that selectively produce mono-functionalized products.^[6]

Several strategies for metal-catalyzed partial oxidation of alkanes have been pursued. Here, we divide these strategies into two categories, those that form catalytic intermediates with metal-carbon bonds and those that generate free alkyl radical intermediates without metal-carbon bond formation. Arguably, the former strategy has been dominated by soluble molecular catalysts wherein the C–H bond can be cleaved by a number of reactions (*e.g.*, oxidative addition, σ -bond metathesis, electrophilic substitution, etc.).^[3c,d,6b,7] Thus, a variety of homogeneous catalysts have been examined for light alkane functionalization, with emphasis on electrophilic metals. Often, electrophilic metal catalysts are believed to function via initial coordination of the alkane followed by proton removal to generate a M–alkyl intermediate, which is then susceptible to a reductive nucleophilic functionalization step (often after oxidation of the metal-alkyl intermediate). For example, the Catalytica system, one of the most effective and well-known electrophilic catalysts, converts methane to methyl bisulfate with high yield and selectivity, >70% and >90%, respectively, using a platinum catalyst (bpym)PtCl₂ (bpym = 2,2'-bipyrimidinyl) in oleum.^[8] Germane here, it has been proposed that the electron-withdrawing nature of the bisulfate group protects methyl bisulfate from over-oxidation by the electrophilic catalyst.^[9] This strategy has been extended to catalysts based on Pd, Au, Hg, Tl and Sb,^[10] and stoichiometric alkane C–H activation with main group elements has been demonstrated recently.^[11] Sulfonation using SO₃ has also been demonstrated to generate methane-sulfonic acid from methane.^[12] However, electrophilic metal catalysts have limitations. For example, they are often inhibited by even weak bases and, thus, often operate effectively only in strongly acidic media (often only in superacids).^[13]

In contrast to the “organometallic” approach for alkane functionalization, which features catalytic intermediates with metal-carbon bonds, many heterogeneous catalysts for light alkane oxidation are thought to operate by homolytic C–H

[a] Dr. N. S. Liebov, Dr. N. Coutard, Dr. S. E. Kalman, Prof. T. B. Gunnoe
Department of Chemistry
University of Virginia
Charlottesville VA 22904 (USA)
E-mail: tbg7h@virginia.edu

[b] Dr. J. M. Goldberg, Dr. N. C. Boaz, T. Zhuang, Prof. J. T. Groves
Department of Chemistry
Princeton University
Princeton NJ 08544 (USA)
E-mail: jtgroves@princeton.edu

[c] Dr. N. C. Boaz
Department of Chemistry
North Central College
Naperville IL 60540 (USA)

[d] Dr. S. E. Kalman
Chemistry Program
School of Natural Sciences and Mathematics
Stockton University
Galloway NJ 08205 (USA)

 Supporting information for this article is available on the WWW under <https://doi.org/10.1002/cctc.201901175>

cleavage to generate free alkyl radicals.^[14] Examples include iron- and copper-based zeolites and transition metal oxides.^[15] These catalysts typically require high temperatures, often >250 °C, and because the rate of reaction is often directly dependent on the strength of C–H bonds, mono-functionalized products are often more reactive than starting alkanes. Thus, although catalytic oxyhalogenation offers a route for light alkane functionalization by converting alkanes to alkyl halides,^[16] the alkyl halide has weaker C–H bonds relative to the starting alkane,^[17] and over-oxidation is significant at high alkane conversions.^[17c,18]

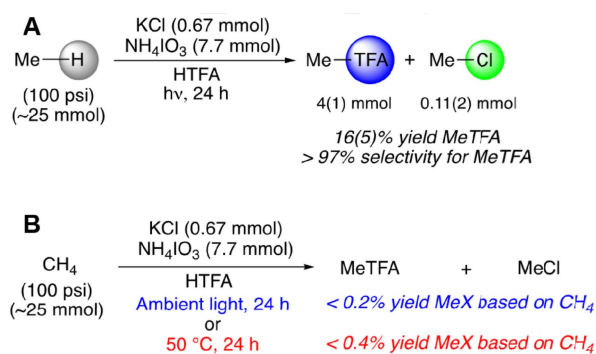
Our groups have previously demonstrated thermal functionalization via oxyesterification (OxE) of light alkanes in trifluoroacetic acid using chloride and iodine oxide salts.^[19] Using iodate as the oxidant, methane, ethane and propane are converted to the corresponding trifluoroacetate esters in high substrate-based yields, ~25% for methane, ~30% for ethane, and ~20% for propane using iodate as the oxidant. The alkyl esters can undergo hydrolysis to generate alcohol and regenerate HTFA. Reactions proceed over a wide range of temperatures (100–235 °C) and pressures (35–1000 psi). Although this thermal OxE process has some similarities to oxychlorination with an oxidant and a chloride source, it exhibits unique selectivity for the mono-functionalized ester product. Recently, combined experimental and computational studies found evidence for a reaction pathway in which free radical intermediates mediate homolytic alkane C–H bond-breaking.^[20] DFT calculations indicated that IO₂[•] and Cl[•] radicals formed *in situ* under OxE conditions (*i.e.*, chloride and iodate or periodate in HTFA) can abstract a hydrogen atom from methane.^[20a] Thus, the reactions are catalytic in chloride, which is a differentiating factor compared to traditional catalytic alkane oxychlorination. In our previous studies, the formation of key reaction intermediates was proposed to depend on the acidity of HTFA. Thus, reactions in acetic acid were less successful. Iodine, which forms *in situ*, was proposed to serve as an efficient alkyl radical trap to generate alkyl iodides that are converted to R-TFA products in HTFA solvent. Importantly, the electron-withdrawing TFA ester functionality was demonstrated to protect the alkyl products from over-oxidation.^[20a,21] Thus, we have proposed that this OxE process is similar to the strategy using electrophilic metals to produce methyl bisulfate in oleum (see above) but is successful in a less acidic solvent (*i.e.*, HTFA vs. oleum).

While there is a significant body of work regarding the functionalization of light alkanes under thermal conditions, photo-mediated partial oxidation of light alkanes has limited precedent.^[22] We speculated that a photo-initiated oxyesterification (photo-OxE) process might offer advantages over the thermal process. For example, oxidation of HTFA is an issue for the OxE process with iodate and chloride, which limits alkyl ester yield,^[19a] and we considered that using lower temperatures with a photo-initiated process might enhance yields of the alkyl ester product by minimizing oxidation of the solvent. Thus, we pursued photolysis as a method to generate reactive intermediates under milder reaction conditions. Herein, we report a photo-OxE process for light alkanes that achieves high alkyl ester and halide yields of ~50% based on methane and ~80%

based on ethane. These yields provide a substantial increase in efficiency compared to the previously reported thermal reactions.

Results and Discussion

From our initial reports of the iodate/chloride OxE process operated under thermal conditions, the highest yield, based on methane, of MeX (X = TFA, Cl) using KCl/NH₄IO₃ was 24%.^[19a] An initial screening of the photochemical reactivity of the OxE process found that high yields relative to alkane (16% MeX relative to methane with a 35:1 ratio of MeTFA:MeCl) could be obtained using a mercury lamp (Scheme 1A). Control reactions



Scheme 1. (A) Photochemical partial oxidation of methane using a mercury lamp. Conditions: CH₄ (100 psi), KCl (0.67 mmol), NH₄IO₃ (7.7 mmol), HTFA (8 mL), 24 h photolysis using the Hg lamp. The percent yield of MeTFA is based on the amount of added methane. The standard deviation is based on a minimum of three experiments. (B) Oxidation of methane using the OxE system under ambient light. Conditions: CH₄ (100 psi), KCl (0.67 mmol), NH₄IO₃ (7.7 mmol), HTFA (8 mL), 24 h exposure to laboratory light in a fume hood or 24 h heating at 50 °C in an oil bath.

using ambient light or heating at 50 °C gave minimal methane functionalization (Scheme 1B). Similar to the previously reported thermal reaction,^[19] the production of ~4 mmol of MeTFA reveals a likely catalytic role for chloride since only 0.67 mmol of KCl are used.

In the absence of chloride, trace MeTFA is produced (Figure 1A). Thus, chloride is essential to the methane functionalization. Increasing the starting chloride amount increases the MeX yield (Figure 1A). MeTFA yields of ~25%, based on methane, with 94% or 91% selectivity for MeTFA, were observed with 2.01 or 3.35 mmol of starting KCl, respectively (selectivity refers to the ratio of MeTFA to MeCl). With higher chloride starting amounts (≥6.7 mmol), the selectivity shifts toward MeCl, and a small amount of undesired over-oxidation to form dichloromethane is observed (Figure 1A). Also, with 6.7 mmol of KCl, the overall yield of MeX (X = TFA or Cl) drops to 20.7(7)%, with selectivity for MeTFA decreasing to 70%. We speculate (see below) that a larger KCl amount allows chlorine to compete with iodine to trap the putative methyl radical, which forms MeCl. Unlike MeI, MeCl is not readily converted to

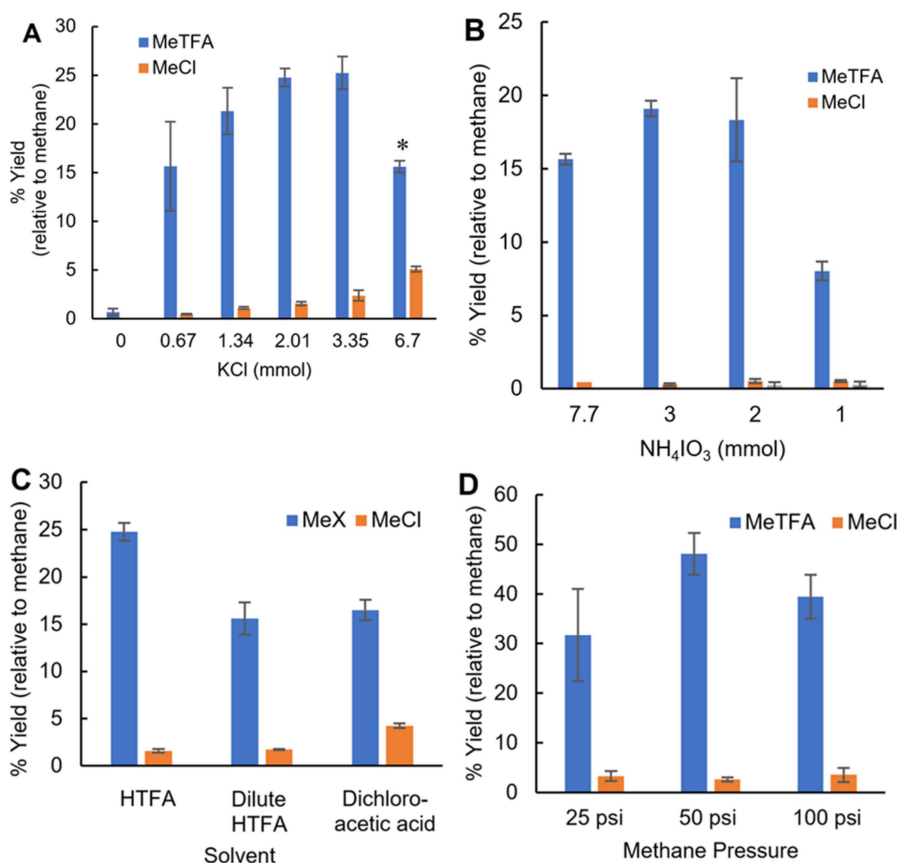


Figure 1. (A) Effect of starting KCl amount on MeX yield. Conditions: CH_4 (100 psi), KCl (0.67–6.7 mmol), NH_4IO_3 (7.7 mmol), HTFA (8 mL), 24 h photolysis using the Hg lamp. Error bars denote standard deviations based on at least three experiments. *With 6.7 mmol, 1.73(2)% yield of dichloromethane is also observed. (B) Effect of starting NH_4IO_3 amount on MeX yield. Conditions: CH_4 (100 psi), KCl (2.01 mmol), NH_4IO_3 (1.0–7.7 mmol), HTFA (8 mL), 24 h photolysis using the Hg lamp. Error bars denote standard deviations based on at least two experiments. (C) Photochemical partial oxidation of methane by KCl/ NH_4IO_3 in different solvent combinations. Dilute HTFA is 3:1 mol:mol HTFA: H_2O . MeX is the corresponding acetate ester for each acid. Conditions: CH_4 (100 psi), KCl (2.01 mmol), NH_4IO_3 (7.7 mmol), solvent (8 mL), 24 h photolysis using the Hg lamp. Error bars denote standard deviations based on at least three experiments. (D) Effect of methane pressure (with longer reaction times) on photochemical OxE of methane. Conditions: CH_4 (25, 50, or 100 psi), KCl (2.01 mmol), NH_4IO_3 (7.7 mmol), HTFA (8 mL), 48 h photolysis using the Hg lamp. Error bars denote standard deviations based on at least three experiments.

MeTFA,^[19a] and, hence, the formation of MeCl likely removes the chlorine catalyst from the reaction.

The effect of varying the amount of NH_4IO_3 was also studied (Figure 1B). Decreasing the amount of NH_4IO_3 from 7.7 mmol resulted in slightly higher yields of MeX relative to methane when using 2 or 3 mmol of the oxidant. However, using 1 mmol of NH_4IO_3 , the yield of MeX was significantly lower.

Longer reaction times and lower methane pressures were tested with the optimal starting KCl amount of 2.01 mmol. With 100 psi methane (~25 mmol of methane), 39(4)% yield of MeTFA was observed after 48 h of photolysis (Figure 1C), higher than optimized yields for $\text{IO}_3^-/\text{Cl}^-$ under thermal conditions (180 °C, 1 h, 24% yield MeX). Also, the product concentration obtained using photolysis is much greater (~1.2 M vs ~0.23 M) than the highest yield for the thermal OxE process obtained with iodate. With 50 psi of methane, a 48(4)% yield of MeTFA was obtained with 95% selectivity. With 25 psi of methane, lower average yields are obtained with higher variability between experiments.

In previously published work, the solvent scope of the thermal OxE process was examined, and it was found that HTFA was the most effective solvent. We also sought to test the influence of the reaction solvent on methane functionalization for the photochemical OxE reaction. While the highest yields of functionalized products are obtained with HTFA, MeX yields (X = TFA or dichloroacetate) of 16(2)% and 17(1)% are obtained after 24 h using dilute HTFA (3:1 mol:mol HTFA: H_2O) and the weaker acid dichloroacetic acid (pK_a 1.35 versus 0.52 for HTFA) respectively, as reaction solvents (Figure 1D). The tolerance of water is notable, as many light alkane functionalization processes in acidic media exhibit poor activity in non-superacidic media. Acetic acid was among those tested as a potential solvent for thermal methane functionalization using the iodate/chloride OxE process. Although MeOAc was produced from the reaction of methane with KCl/ NH_4IO_3 in HOAc, under thermal conditions it was demonstrated that MeOAc originates from oxidation of HOAc rather than methane functionalization. However, only trace MeOAc, ~0.1% based on methane, is observed for the photo-OxE reaction with methane, indicating

that solvent oxidation is minimal under these milder conditions. This lends evidence that the photolysis conditions reduce the extent of solvent oxidation (compared to thermal reactions), which might be responsible for the higher yields of MeOAc under thermal conditions. Further, the inability of acetic acid to facilitate methane functionalization could indicate that it is too weakly acidic to generate the necessary active species, which is consistent with our previous studies. Previous UV/Vis spectroscopy of reaction mixtures indicated that an acidic solvent is required to generate Cl_2 and interhalogen species (*i.e.*, ICl and/or ICl_3) that are expected to be precursors of active intermediates in the functionalization process. HTFA, the effective solvent in the thermal $\text{KCl}/\text{NH}_4\text{IO}_3$ system, generates these species *in situ*, but HOAc does not.

To test the ability of visible light to functionalize methane, irradiation using a compact fluorescent light (CFL) was examined. As shown in Figure 2, irradiation with a 105 W CFL results

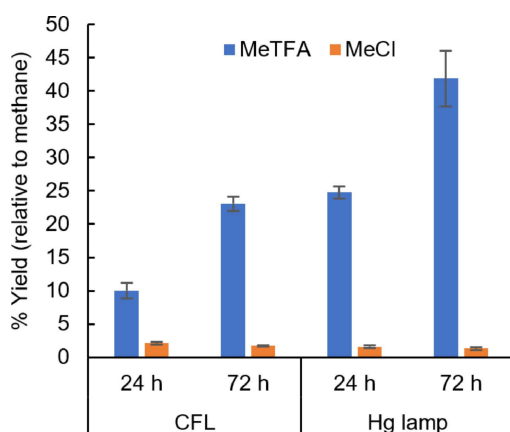


Figure 2. Comparison of irradiation by a mercury lamp and a 105 W compact fluorescent light (CFL) for photochemical partial oxidation of methane by $\text{KCl}/\text{NH}_4\text{IO}_3$. Conditions: CH_4 (100 psi), KCl (2.01 mmol), NH_4IO_3 (7.7 mmol), solvent (8 mL), 24 h photolysis. Error bars denote standard deviations based on at least three experiments.

in methane functionalization; however, yields are lower than those obtained with the mercury lamp. After 24 h of irradiation, ~10% yield of MeTFA is obtained using the 105 W CFL, while ~25% yield is obtained with the mercury lamp. After 72 h, 105 W CFL irradiation generates MeTFA in ~25% yield, but reaction times longer than 72 h do not result in improved yields of MeX.

Photo-OxE reactions of ethane and propane were also examined using the $\text{KCl}/\text{NH}_4\text{IO}_3$ mixture in HTFA with the mercury lamp. For ethane, the selectivity for EtTFA and EtCl is high with minimal formation of the di-functionalized products 1-iodo-2-trifluoroacetoxyethane, 1-chloro-2-trifluoroacetoxyethane, 1,2-bis(trifluoroacetoxy)ethane and 1,2-dichloroethane (Figure 3). Using 25 psi of ethane, an optimized EtX ($\text{X}=\text{TFA}$ or Cl) yield of 82(5)% was demonstrated. There is also evidence for a 1,1-difunctionalized product at low ethane pressures by ^1H NMR spectroscopy and from the $^1\text{H},^1\text{H}$ -COSY spectrum (Figur-

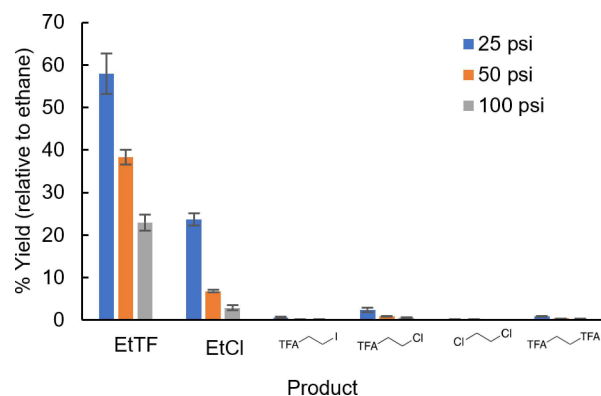


Figure 3. Photochemical functionalization of ethane with $\text{KCl}/\text{NH}_4\text{IO}_3$. Conditions: CH_3CH_3 (25, 50 or 100 psi), KCl (2.01 mmol), NH_4IO_3 (7.7 mmol), HTFA (8 mL), 24 h photolysis using the Hg lamp. Error bars denote standard deviations based on three experiments.

es S5 and S6). There is coupling between a doublet at 1.72 ($J=5.8$ Hz) and a quartet at 6.39 ppm ($J=5.8$ Hz), which is similar to the reported resonances for 1,1-bis(trifluoroacetoxy)ethane. Assuming the doublet corresponds to a methyl peak, there is a 1.6(8)% yield of this product relative to ethane with 25 psi, with only trace formation observed under 50 or 100 psi of ethane. These observations suggest that at high conversions of alkane, over-oxidation occurs but only to a very minimal degree. Similarly, in addition to the major product, 2-trifluoroacetoxypropane, a variety of products, including di-functionalized propyl products, are generated in the photochemical oxidation of propane (Figure 4).

Periodate was also examined as an oxidant for the photochemical process (Figure 5). Although similar MeTFA yields were

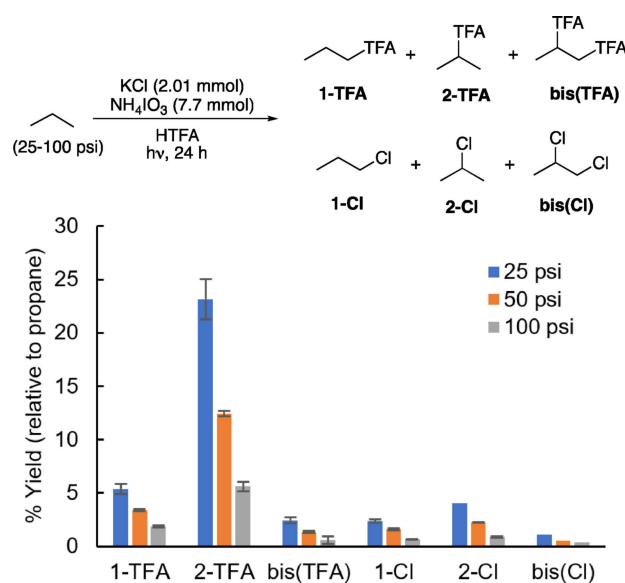


Figure 4. Photochemical functionalization of propane (25–100 psi) with KCl (2.01 mmol) and NH_4IO_3 (7.7 mmol) in HTFA with 24 h of photolysis using the Hg lamp. Error bars denote standard deviations based on three experiments.

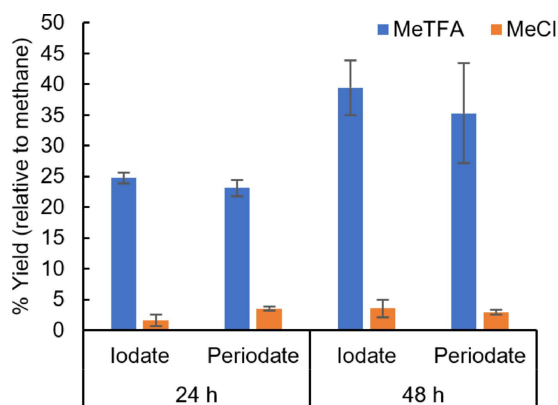
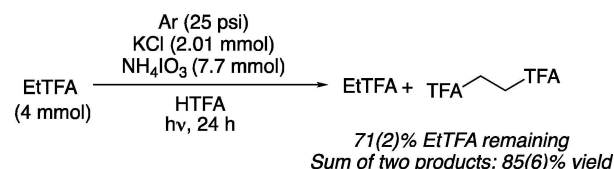


Figure 5. Comparison of photochemical functionalization of methane with iodate versus periodate. Conditions: CH_4 (100 psi), KCl (2.01 mmol), NH_4IO_3 or KIO_4 (7.7 mmol), HTFA, (8 mL), 24 or 48 h photolysis using the Hg lamp. Error bars denote standard deviations based on three trials for each condition except for the 48 h trial with periodate, which is based on six trials.

obtained using either iodate or periodate, the standard deviations associated with MeTFA were greater when using periodate.

In previous studies we found that the thermal OxE chemistry likely operates by a radical process involving H-atom abstraction from alkanes, resulting in the selective formation of alkyl trifluoroacetates in HTFA. The alkyl trifluoroacetates were demonstrated experimentally to be stable under the OxE reaction conditions, minimizing over-oxidation and consequently enabling high yields and selectivities. Thus, we sought to determine and compare the rates of methane functionalization and MeTFA decay under photolysis.

MeTFA was found to be stable under photochemical conditions in the presence of iodate and chloride. Figure 6 shows a comparison of methane functionalization and MeTFA decomposition under the conditions optimized for methane functionalization. The stability of MeTFA indicates the poten-



Scheme 2. EtTFA decay in the presence of KCl , NH_4IO_3 and HTFA after 24 h photolysis using the Hg lamp.

tially broad applicability of the ester protection strategy beyond the initial thermal conditions. The rates of methane functionalization and MeTFA decay cannot be compared directly as the concentration of methane in HTFA solution is unknown. However, to approximate the relative rate of methane functionalization versus MeTFA decay, the slopes of product vs time plots were compared. As the plot for methane functionalization is linear through 24 h, the fit of the points through the first 24 h was used to obtain the slope for functionalization (Figure S11). All of the data points for MeTFA decay were used to obtain a linear fit of those results. The selectivity for methane functionalization vs. MeTFA decay is 13, similar to the ratio observed in the thermal process, 13.5. Although the rate of EtTFA oxidation was not quantified, EtTFA was also found to be stable after 24 h of photolysis (Scheme 2).

We speculate that chlorine radical is an important intermediate in the photo-OxE process. *N*-chlorosuccinimide (NCS) was used to compare the photo-OxE process to a traditional radical-based functionalization method. With benzoyl peroxide as a radical initiator, the photolysis of methane with NCS generates MeCl and dichloromethane. However, upon addition of iodine to the system, MeTFA is produced (Scheme 3), similar to observations reported for the thermal process.^[19] Mel has also been demonstrated to convert rapidly to MeTFA under the photochemical conditions (Scheme 4). Thus, this result is consistent with chlorine-mediated formation of methyl radical, iodine trapping to form Mel, and conversion of Mel in HTFA to

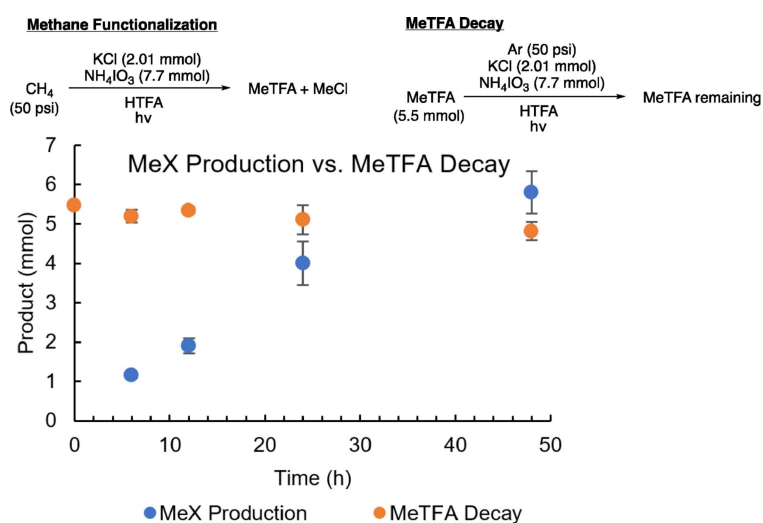
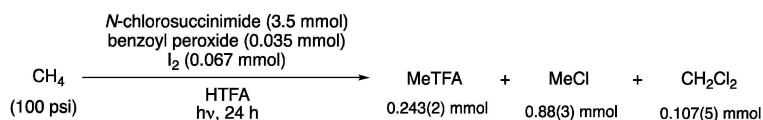
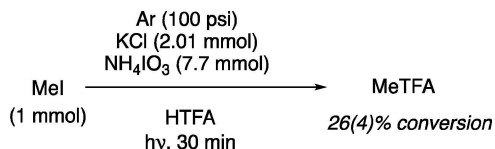


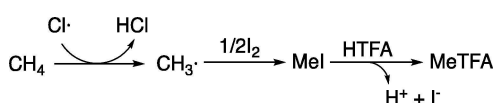
Figure 6. Methane functionalization vs. MeTFA decay in the presence of KCl , NH_4IO_3 and HTFA under photochemical reaction conditions as a function of time.



Scheme 3. Addition of iodine to chlorination by *N*-chlorosuccinimide and benzoyl peroxide results in formation of MeTFA under photolysis using the Hg lamp. Standard deviations are based on at least three experiments.



Scheme 4. MeI conversion to MeTFA under photolysis using the Hg lamp. The standard deviation is based on at least three experiments.



Scheme 5. Methane functionalization by chlorine radical wherein the methyl radical formed following H-atom abstraction is trapped by iodine to generate MeI, which is converted to MeTFA in HTFA solvent.

MeTFA (Scheme 5). While it is possible that functionalization occurs through a carbocationic reaction pathway, we believe it is unlikely under our reaction conditions.¹² These data demonstrate that iodine is likely an efficient radical trap in the photochemical process, similar to the thermal process. Over-oxidation to form dichloromethane is also suppressed when iodine is added. For example, without added iodine, dichloromethane accounts for 25% of functionalized products, but <9% of products are due to dichloromethane when 0.067 mmol of I₂ is added. The addition of iodine to the photochemical iodate/chloride reaction mixture was examined and did not result in improved yields (see Supporting Information, Figure S14).

Since we observed a significant improvement in product conversion under photo-OxE conditions compared to thermal reactivity, we were interested in probing possible mechanistic differences between the thermal and photo-initiated reactions. We previously examined kinetic isotope effects (KIE) for thermal OxE using adamantane-*h*₁₆/*d*₁₆ [*k*_H/*k*_D = 1.52(3)] as a model system for methane. However, at room temperature, adamantane is poorly soluble in HTFA, rendering interpretation of KIE experimental results ambiguous. Instead, we examined cyclohexane-*h*₁₂/*d*₁₂ under the new photochemical conditions and also subjected these substrates to thermal OxE conditions to provide a direct comparison. We used cyclohexane as a model substrate for our KIE studies since we can more easily control stoichiometric reactions and the C–H bond dissociation energy (BDE) for cyclohexane (99.5 kcal mol⁻¹) is quite similar to the light alkanes propane (100.9 kcal mol⁻¹ for –CH₃ and 98.1 kcal mol⁻¹ for –CH₂–) and ethane (100.5 kcal mol⁻¹). A caveat here is that the mechanistic conclusions from our

cyclohexane studies might not directly translate to methane due to its higher C–H BDE (~105 kcal mol⁻¹).

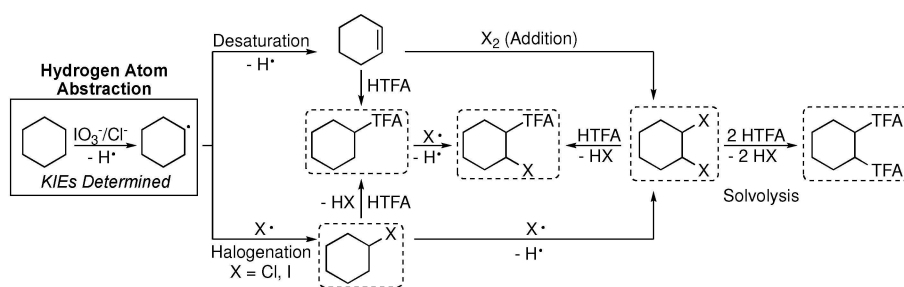
We screened cyclohexane functionalization under stoichiometric conditions with equimolar substrate and NH₄IO₃ oxidant. Under thermal conditions (100 °C, 1 h), functionalization of cyclohexane with 1 equiv. of NH₄IO₃ and 0.25 equiv. of KCl, relative to cyclohexane, in HTFA solvent results in the formation of five products as detected by GC-MS. The observed mono-functionalized products were cyclohexyl-TFA and cyclohexyl-chloride, which likely result from a hydrogen atom abstraction pathway. We hypothesize that the three di-functionalized products result from initial desaturation of cyclohexane to give cyclohexene, and that addition of *in situ*-generated Cl₂, ICl or ICl₃ across the double bond in cyclohexene yields a dihalocyclohexane intermediate; the detection of *trans*-1,2-dichlorocyclohexane as a stable product in one of these reactions corroborates this hypothesis. Solvolysis of the dihalo intermediate by HTFA yields both 1,2-bis(trifluoroacetoxy)cyclohexane and 2-chloro-1-trifluoroacetoxy-cyclohexane, as detected by GC-MS and ¹H NMR spectroscopy (Scheme 6).

Other light sources were also examined (Table 1). The 105 W CFL gave similar results to the 26 W CFL, with ~25% yield of functionalized products based on cyclohexane (Table S1 in the Supporting Information provides results under additional conditions). Use of a Rayonet UV Photochemical Reactor (UV-reactor) gave further improved yields, 45(2)%, similar to the best yields obtained with methane under optimized conditions. The reaction time using the UV-reactor was limited to 18 h due to the build-up of pressure under reaction conditions.

Table 1. Cyclohexane functionalization under OxE conditions (thermal and photochemical).^[a]

	$\text{C}_6\text{H}_{12} \xrightarrow[\text{HTFA, 2 mL}]{\begin{array}{l} \text{KCl (0.13 mmol)} \\ \text{NH}_4\text{IO}_3 \text{ (0.5 mmol)} \end{array}} \text{C}_6\text{H}_{11}\text{R}^1 + \text{C}_6\text{H}_{10}\text{R}^1\text{R}^2$ (0.5 mmol) thermal or photochemical			
	100 °C 1 h	26 W CFL 24 h	105 W CFL 24 h	UV-reactor 18 h
R ¹ = TFA	2.7(8)	13.3(3)	11.7(6)	30(2)
R ¹ = Cl	1.6(1)	4.5(1)	4.7(3)	ND
R ¹ = R ² = TFA	trace	1.1(1)	1.3(1)	4.7(2)
R ¹ = R ² = Cl	trace	1.6(1)	2.2(3)	ND
R ¹ = Cl; R ² = TFA	trace	*6.4(3)	*5.6(3)	*10.1(5)
Total Product Yield	4.3(8)	26.9(5)	25.5(8)	45(2)

[a] Product yields (%) are shown. Products were quantified using GC-MS vs. an internal standard (tetradecane). *Denotes detection and quantification by ¹H NMR spectroscopy. ND = not detected.



Scheme 6. Proposed synthetic routes to products from cyclohexane functionalization. Products in dotted boxes were detected and quantified by GC-MS and/or ^1H NMR spectroscopy for $X = \text{Cl}$ only. It is proposed that for $X = \text{I}$, the compounds readily undergo solvolysis by HTFA or exchange with Cl^- so the alkyl iodides are not detected.

Since a significant amount of difunctionalized product was observed under both thermal and photochemical pathways, multiple reactive pathways could be occurring simultaneously. However, it is still possible to make a reasonable estimate of the isotope effect since we are only probing the initial hydrogen atom abstraction of cyclohexane (Scheme 6). To compare the two pathways, we examined the ratio of the combined protiated products vs. the combined deuterated products ($k_{\text{H}}/k_{\text{D}}$, Table 2). The thermal iodate/chloride system gave a $k_{\text{H}}/k_{\text{D}}$ of

We previously showed that upon combining iodate and chloride in HTFA, Cl_2 and ICl/ICl_3 could be detected by UV-vis spectroscopy (see Supporting Information Figure S39). To probe if chlorine atoms were intermediates in our photochemical iodate/chloride system, we also examined the $k_{\text{H}}/k_{\text{D}}$ values for reactions of cyclohexane- h_{12}/d_{12} with ICl , ICl_3 , and periodate/chloride, and compared those to the iodate/chloride system and the reported Cl_2 reaction (see Supporting Information for stoichiometric reaction yields). By UV-vis spectroscopy, it has been demonstrated that combining periodate and chloride in HTFA also gives Cl_2 and ICl/ICl_3 (see Supporting Information, Figure S38), albeit at much lower concentrations than analogous conditions with iodate. Examination of the thermal $k_{\text{H}}/k_{\text{D}}$ values for reaction of ICl_3 ($k_{\text{H}}/k_{\text{D}} = 2.3(2)$) and periodate/chloride ($k_{\text{H}}/k_{\text{D}} = 1.94(3)$) with cyclohexane gave similar isotope effects to iodate/chloride ($k_{\text{H}}/k_{\text{D}} = 2.1(2)$). However, the $k_{\text{H}}/k_{\text{D}}$ for the thermal reaction of ICl with cyclohexane gave a more significant $k_{\text{H}}/k_{\text{D}}$ of 4.3(1). These results indicate that the thermal reaction is not consistent with solely a chlorine atom abstraction pathway.

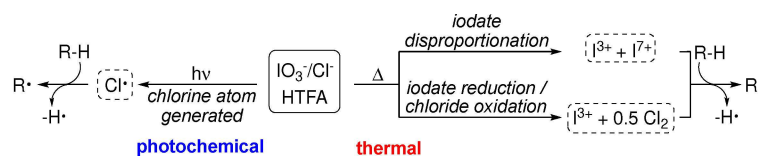
Since certain thermal $k_{\text{H}}/k_{\text{D}}$ values (entries 1–3, Table 2) were in line with each other, we hypothesize that these species arise from the same mechanistic intermediate. Therefore, we propose a scenario where iodate disproportionates into I(III) and I(VII) species that are both able to facilitate hydrogen atom abstraction (Scheme 7). As we previously reported, the calculated intermediate IO_2^\bullet may be an *in situ* generated active species. Alternatively, iodate might be reduced with subsequent oxidation of chloride to generate Cl_2 and an I(III) species. In either scenario, given the $k_{\text{H}}/k_{\text{D}}$ of 4.3(1) for ICl with cyclohexane, we do not expect a significant iodine(I) component. In contrast, the $k_{\text{H}}/k_{\text{D}}$ values for photochemical cyclohexane functionalization by iodate/chloride, periodate/chloride, ICl and ICl_3 are nearly identical to the reported Cl_2 system ($k_{\text{H}}/k_{\text{D}} \approx 1.1\text{--}1.2$), indicating the possibility that the photo-OxE process operates exclusively through hydrogen atom abstraction by a chlorine atom. Since ICl , ICl_3 and Cl_2 are all observed upon combining iodate and chloride in HTFA, any of these species could serve as chlorine atom sources.

Table 2. OxE kinetic isotope effect experiments with cyclohexane under thermal and photochemical conditions.^[a]

Entry	Thermal/ Photochemical	Condition	$k_{\text{H}}/k_{\text{D}}$ ^[b]
1	Thermal	$\text{KCl}/\text{NH}_4\text{IO}_3$	2.1(2); 1.9(1) ^[c]
2		KCl/KIO_4	1.94(3); [2.2(1)] ^[c]
3		ICl_3	2.3(2)
4	Photochemical	ICl	4.3(1)
5		$\text{KCl}/\text{NH}_4\text{IO}_3$	1.06(3)
6		KCl/KIO_4	1.08(3)
7		ICl_3	1.15(1)
8		ICl	1.21(4)

[a] Conditions: NH_4IO_3 (0.25 mmol), KCl (0.14 mmol); KIO_4 (0.25 mmol), KCl (0.14 mmol); ICl_3 (0.25 mmol); ICl (0.28 mmol), [b] $k_{\text{H}}/k_{\text{D}}$ ratios reflect total protiated vs. total deuterated products, [c] KIE reaction performed at 130 °C, 1 h. Product ratios were determined by GC-MS. Standard deviations are based on at least three experiments.

2.1(2), which differs from the $k_{\text{H}}/k_{\text{D}}$ of the photochemical reaction ($k_{\text{H}}/k_{\text{D}} = 1.06(3)$), suggesting two different reaction mechanisms. Previous work by Li and Pirasteh found a $k_{\text{H}}/k_{\text{D}}$ of 1.14(1) for the reaction of atomic chlorine with cyclohexane- h_{12}/d_{12} , in line with our photo-OxE cyclohexane functionalization. While the thermal iodate/chloride yields are low for cyclohexane functionalization, the $k_{\text{H}}/k_{\text{D}}$ values did not significantly change upon increasing the temperature from 100 to 130 °C indicating that the reactive species is not readily affected by a change in temperature (Table 2).



Scheme 7. Proposed species resulting from thermal or photochemical iodate/chloride mixtures in HTFA. For each condition, any of the species in dotted boxes may facilitate hydrogen atom abstraction from an alkane.

Conclusions

The photo-OxE process for light alkanes with iodate-chloride mixtures is selective for partial oxidation products using chloride as catalyst. The yields for methane and ethane (~50% and 80%, respectively) are notable for a process that likely involves homolytic hydrogen atom abstraction. The photochemical process exhibits tolerance to water and weaker acid solvents, but yields are highest when using neat HTFA as the solvent. Generally, the new photo-reaction yields are higher than those obtained using the same reaction under thermal conditions (*i.e.*, optimal yields of 24% and ~50% for thermal and photochemical reactions, respectively), which could be due to the reduction of reactive intermediates under the photochemical conditions. The higher yields could also be the result of a reduction of solvent oxidation under the milder photochemical conditions.

Investigation into the mechanism indicates a chlorine atom abstraction radical pathway for the photochemical process, which differs from the thermal pathway where multiple active species may be present. When iodine is added to the methane chlorination reaction with *N*-chlorosuccinimide and benzoyl peroxide, MeTFA is generated. In the absence of iodine, MeTFA is not produced. This demonstrates iodine's efficiency as a radical trap, as even with a large excess of a chlorine radical source, MeI can be generated *in situ*, similar to what was observed thermally. The addition of chloride is necessary, and slight increases in chloride concentration has a beneficial effect on product yield. However, the use of high concentrations of KCl result in lower yields of functionalized product, potentially due to the ability of chlorine radical to trap active intermediates and remove the catalytic amount of chlorine from the cycle. The stability and protecting effect of the product ester group that was found under thermal conditions is also transferable to the photochemical system.

Experimental Section

Caution: Many of the reagents and conditions described herein are potentially hazardous. Appropriate safety procedures should be consulted prior to handling concentrated acids, strong oxidants, and mixtures of hydrocarbon substrates and oxygen, especially under pressure.

General Comments and Materials. All reactions were carried out under ambient atmosphere unless indicated otherwise. Potassium chloride, ammonium iodate, potassium periodate, iodine, iodine trichloride, iodine monochloride, trifluoroacetic acid, glacial acetic

acid, dichloroacetic acid, benzene- d_6 , nitromethane, benzoyl peroxide, methyl trifluoroacetate, cyclohexane, and cyclohexane- d_{12} were purchased commercially and used as received. *N*-Chlorosuccinimide was purchased commercially and recrystallized from glacial acetic acid prior to use. Methane, ethane, propane and argon were purchased from GTS-Welco and used as received. The mercury lamp (Hanovia, medium pressure, UV lamp, 450 W) was purchased from Ace Glass and used as received. The 105 W compact fluorescent lightbulb (Overdrive CFL, 420 W equivalent, 5000 K full spectrum) was purchased from Amazon and used as received. The 26 W CFL (2700 K) was purchased from Grainger and used as received. The UV reactor is a Rayonet Photochemical Reactor (RPR-100) containing six 8 watt RPR2537 A low pressure mercury lamps. Fisher-Porter reactors were purchased from Andrews Glass and used with custom-built Swagelok reactor tops. ^1H NMR spectra were recorded on a Varian Inova 500, Bruker Avance 500, Avance DRX 600 or an Avance III 600 spectrometer. NMR spectra were obtained using neat reaction mixtures with C_6D_6 inserted in a sealed capillary tube as an internal lock reference. Chemical shifts are reported relative to the added internal standard (δ 4.18 for nitromethane, 2.04 for glacial acetic acid, or 7.26 for chloroform). GC-MS analysis was performed using an Agilent Technologies 7890 A gas chromatograph equipped with a fused silica column (crossbond 35% diphenyl-65% dimethyl polysiloxane; 30 m \times 0.32 mm; 0.5 μm thickness) and electron impact mass analyzer.

General procedure for photochemical oxidation of light alkanes. A Fisher-Porter reactor was charged with a stir bar, potassium chloride, ammonium iodate and HTFA (8 mL). The reactor was then sealed and pressurized with alkane. The reactor was then placed on a stir plate 13 cm away from the lamp and stirred. The Hg lamp was in a closed chamber for safety purposes. Following the reaction, the lamp was turned off, and the reactor was vented. Internal standard was then added to the reaction mixture, and the reaction mixture was stirred. An aliquot was removed for centrifugation, and the supernatant was used for ^1H NMR analysis. Similar procedures were used for the other light sources.

MeTFA decay under photochemical conditions. A Fisher-Porter reactor was charged with a stir bar, potassium chloride (2.01 mmol), ammonium iodate (7.7 mmol), MeTFA (5.37 mmol) and HTFA (8 mL). The reactor was sealed and pressurized with argon. The reactor was then placed on a stir plate in front of the Hg lamp and stirred in the chamber, which was closed before turning the lamp on. Following the reaction, the lamp was turned off, and the reactor was vented. Internal standard was added to the reaction mixture, and the mixture was stirred. An aliquot was removed for centrifugation, and the supernatant was used for ^1H NMR analysis.

Chlorination using *N*-chlorosuccinimide and benzoyl peroxide. A Fisher-Porter reactor was charged with a stir bar, recrystallized *N*-chlorosuccinimide (3.5 mmol), benzoyl peroxide (0.035 mmol), and HTFA (8 mL) in the glovebox. If used, iodine (0.067 mmol) was also added to the reactor. HTFA was heated to reflux for 1 h under N_2 before being added to the reactor. The reactor was then sealed and pressurized with 100 psi of methane. The reactor was placed on a stir plate in front of the lamp and set to stir in the Hg lamp

chamber, which was closed before turning the lamp on. Following the reaction, the lamp was turned off and the reactor was vented. Internal standard was added to the reaction mixture, and the mixture was stirred. An aliquot was removed and used for ^1H NMR analysis. Centrifugation was not required as the mixture was homogeneous.

Functionalization of cyclohexane. An 8 mL microwave vial was charged with 98 mg (0.51 mmol) NH_4IO_3 and 10 mg (0.13 mmol) KCl. HTFA (2 mL) and cyclohexane (54 μL , 0.5 mmol) were added to the vial, generating a golden yellow mixture. The vial was sealed with a crimp cap containing a septum. **Thermal:** the vial was placed in an oil bath preheated to 100 $^\circ\text{C}$ and heated for 1 h with vigorous stirring. The vial was then allowed to cool to room temperature. The reaction mixture appeared as a golden yellow solution with abundant white solid. **Photochemical:** the vial was placed in front of the corresponding light source (~ 3 cm) and allowed to stir at room temperature for 24 h unless otherwise specified. After 24 h, the reaction mixture appeared as a magenta solution with white solid. **Workup:** the reaction mixture was removed from the vial and filtered through a PTFE filter into a vial containing tetradecane (0.24 mmol). The reaction vial was rinsed with dichloromethane (5 mL) and filtered. The solutions were combined and washed two times with 10 mL H_2O . The organic layer was isolated and dried over MgSO_4 . An aliquot was taken from the dichloromethane solution and analyzed by GC-MS to quantify cyclohexyl-TFA, cyclohexyl-chloride, 1,2-bis(trifluoroacetoxy)cyclohexane, and 1,2-dichlorocyclohexane vs. tetradecane as the internal standard. The solvent was removed from the dichloromethane solution and the residue was dissolved in CDCl_3 for analysis and quantification of 2-chloro-1-trifluoroacetoxy-cyclohexane by ^1H NMR spectroscopy. Reactions were run in triplicate for each set of conditions.

Kinetic isotope effect studies. An 8 mL microwave vial was charged with 52 mg (0.27 mmol) NH_4IO_3 and 10 mg (0.14 mmol) KCl, 57 mg KIO_4 (0.25 mmol) and 10 mg KCl (0.14 mmol), 58 mg ICl_3 (0.25 mmol), or 45 mg ICl (0.28 mmol). HTFA (2 mL), cyclohexane- h_{12} (27 μL , 0.25 mmol), and cyclohexane- d_{12} (27 μL , 0.25 mmol) were added to the vial. The vial was sealed with a crimp cap containing a septum. The reaction mixture was subjected either to thermal or photochemical reaction conditions as described above. The reaction mixture was removed from the vial and filtered through a PTFE filter. The reaction vial was rinsed with dichloromethane (5 mL) and filtered. The solutions were combined and washed two times with 10 mL H_2O . The organic layer was isolated and dried over MgSO_4 . An aliquot was taken from the dichloromethane solution and analyzed by GC-MS. Reactions were run in triplicate for each set of conditions.

Acknowledgements

This research was sponsored by the U.S. Department of Energy, Office of Energy Efficiency and Renewable Energy, Advanced Manufacturing Office, under contract DE-AC05-00OR22725 with UT-Battelle, LLC. Preliminary research by N.C.B. and T.Z. was supported by the U.S. National Science Foundation award CHE-1464578 to J.T.G.

Conflict of Interest

The authors declare no conflict of interest.

Keywords: methane · C–H functionalization · photochemistry · catalysis · oxidation

- [1] a) Q. Wang, X. Chen, A. N. Jha, H. Rogers, *Renewable Sustainable Energy Rev.* **2014**, *30*, 1–28; b) BP Statistical Review of World Energy 2014, British Petroleum, London, **2014**.
- [2] G. A. Olah, Á. Molnár, in *Hydrocarbon Chemistry*, 2nd ed., John Wiley & Sons, **2003**.
- [3] a) Z. Zakaria, S. K. Kamarudin, *Renewable Sustainable Energy Rev.* **2016**, *65*, 250–261; b) J. A. Martens, A. Bogaerts, N. De Kimpe, P. A. Jacobs, G. Marin, K. Rabaey, M. Saeys, S. Verhelst, *ChemSusChem* **2017**, *10*, 1039–1055; c) N. J. Gunsalus, A. Koppaka, S. H. Park, S. M. Bischof, B. G. Hashiguchi, R. A. Periana, *Chem. Rev.* **2017**, *117*, 8521–8573; d) R. H. Crabtree, *Chem. Rev.* **1995**, *95*, 987–1007; e) P. Schwach, X. Pan, X. Bao, *Chem. Rev.* **2017**, *117*.
- [4] M. S. Matar, M. J. Mirbach, H. A. Tayim, in *Catalysis in Petrochemical Processes*, Kluwer Academic Publishers, Boston, MA, **1988**.
- [5] X. Meng, X. Cui, N. P. Rajan, L. Yu, D. Deng, X. Bao, *Chem.* **2019**, *5*, 1–30.
- [6] a) F. Schuth, *Science* **2019**, *363*, 1282–1283; b) A. Caballero, P. J. Pérez, *Chem. Soc. Rev.* **2013**, *42*, 8809–8820.
- [7] a) T. B. Gunnoe, in *Physical Inorganic Chemistry: Reactions, Processes, and Applications* (Ed.: A. Bakac), John Wiley & Sons, Hoboken, New Jersey, **2010**, pp. 495–549; b) B. G. Hashiguchi, S. M. Bischof, M. M. Konnick, R. A. Periana, *Acc. Chem. Res.* **2012**, *45*, 885–898; c) E. G. Chepaikin, *Russ. Chem. Rev.* **2011**, *80*, 363–396.
- [8] R. A. Periana, D. J. Taube, S. Gamble, H. Taube, T. Satoh, H. Fujii, *Science* **1998**, *280*, 560–564.
- [9] M. Ahlquist, R. J. Nielsen, R. A. Periana, W. A. Goddard, III., *J. Am. Chem. Soc.* **2009**, *131*, 17110–17715.
- [10] a) C. J. Jones, D. Taube, V. R. Ziatdinov, R. A. Periana, R. J. Nielsen, J. Oxgaard, W. A. Goddard, *Angew. Chem. Int. Ed.* **2004**, *116*, 4726–4729; b) R. A. Periana, D. J. Taube, E. R. Evitt, D. G. Löffler, P. R. Wentreck, G. Voss, T. Masuda, *Science* **1993**, *259*, 340–343; c) B. G. Hashiguchi, M. M. Konnick, S. M. Bischof, S. J. Gustafson, D. Devarajan, N. Gunsalus, D. H. Ess, R. A. Periana, *Science* **2014**, *343*, 1232–1237; d) L. C. Kao, A. C. Hutson, A. Sen, *J. Am. Chem. Soc.* **1991**, *113*, 700–701; e) A. Koppaka, S. H. Park, B. G. Hashiguchi, N. Gunsalus, C. R. King, M. M. Konnick, D. H. Ess, R. A. Periana, *Angew. Chem. Int. Ed.* **2019**, *58*, 2241–2245; f) Z. An, X. Pan, X. Y. Liu, X. Han, X. Bao, *J. Am. Chem. Soc.* **2006**, *128*, 16028–16029; g) N. Basickes, T. E. Hogan, A. Sen, *J. Am. Chem. Soc.* **1996**, *118*, 13111–13112; h) A. Sen, M. A. Benvenuto, M. R. Lin, A. C. Hutson, N. Basickes, *J. Am. Chem. Soc.* **1994**, *116*, 998–1003; i) M. Muehlhofer, T. Strassner, W. A. Herrmann, *Angew. Chem. Int. Ed.* **2002**, *41*, 1745–1747; *Angew. Chem.* **2002**, *114*, 1817–1819.
- [11] a) J. S. J. Hargreaves, G. J. Hutchings, R. W. Joyner, S. H. Taylor, *Appl. Catal. A* **2002**, *227*, 191–200; b) J. Li, S. Zhou, J. Zhang, M. Schlangen, D. Usharani, S. Shaik, H. Schwarz, *J. Am. Chem. Soc.* **2016**, *138*, 11368–11377.
- [12] a) V. A. Roytman, D. A. Singleton, *Science* **2019**, *364*; b) C. Diaz-Urrutia, T. Ott, *Science* **2019**, *363*, 1326–+.
- [13] a) B. L. Conley, W. J. Tenn, K. J. H. Young, S. K. Ganesh, S. K. Meier, V. R. Ziatdinov, O. Mironov, J. Oxgaard, J. Gonzales, W. A. Goddard, R. A. Periana, *J. Mol. Catal. A: Chem* **2006**, *251*, 8–23; b) T. Zimmermann, M. Soorholtz, M. Bilke, F. Schuth, *J. Am. Chem. Soc.* **2016**, *138*, 12395–12400.
- [14] R. Horn, R. Schlögl, *Catal. Lett.* **2015**, *145*, 23–39.
- [15] a) J. R. Webb, T. Bolaño, T. B. Gunnoe, *ChemSusChem* **2011**, *4*, 37–49; b) B. E. R. Snyder, M. L. Bols, R. A. Schoonheydt, B. F. Sels, E. I. Solomon, *Chem. Rev.* **2018**, *118*, 2718–2768; c) P. Tomkins, M. Ranocchiaro, J. A. van Bokhoven, *Acc. Chem. Res.* **2017**, *50*, 418–425; d) M. Dusselier, M. E. Davis, *Chem. Rev.* **2018**, *118*, 5265–5329.
- [16] a) J. A. Labinger, *J. Mol. Catal. A* **2004**, *220*, 27–35; b) G. Zichittella, V. Paunovic, A. P. Amrute, J. Perez-Ramirez, *ACS Catal.* **2017**, *7*, 1805–1817; c) V. Paunović, G. Zichittella, P. Hemberger, A. Bodi, J. Pérez-Ramírez, *ACS Catal.* **2019**, *9*, 1710–1725; d) S. G. Podkolzin, E. E. Stangland, M. E. Jones, E. Peringer, J. A. Lercher, *J. Am. Chem. Soc.* **2007**, *129*, 2569–2576.
- [17] a) E. Tschuikow-Roux, S. Paddison, *Int. J. Chem. Kinet.* **1987**, *19*, 15–24; b) A. Fattahi, R. E. McCarthy, M. R. Ahmad, S. R. Kass, *J. Am. Chem. Soc.* **2003**, *125*, 11746–11750; c) A. Breed, M. F. Doherty, S. Gadewar, P. Grosso, I. M. Lorkovic, E. W. McFarland, M. Weiss, *Catal. Today* **2005**, *106*, 301–304.
- [18] a) M. C. Sze, H. Riegel, H. D. Schindler, The Lummus Company, US4207268A, **1980**; b) J. L. Dunn Jr., B. Posey Jr., Dow Chemical

- Company, US2866830A, 1958; c) J. F. Hartwig, *J. Am. Chem. Soc.* **2016**, *138*, 2–24.
- [19] a) G. C. Fortman, N. C. Boaz, D. Munz, M. M. Konnick, R. A. Periana, J. T. Groves, T. B. Gunnoe, *J. Am. Chem. Soc.* **2014**, *136*, 8393–8401; b) S. E. Kalman, D. Munz, G. C. Fortman, N. C. Boaz, J. T. Groves, T. B. Gunnoe, *Dalton Trans.* **2015**, *44*, 5294–5298.
- [20] a) R. Fu, R. J. Nielsen, N. S. Liebov, W. A. Goddard III, T. B. Gunnoe, J. T. Groves, *J. Phys. Chem. C* **2019**, *123*, 15674–15684; b) N. A. Schwartz, N. C. Boaz, S. E. Kalman, T. Zhuang, J. M. Goldberg, R. Fu, R. J. Nielsen, W. A. Goddard III, J. T. Groves, T. B. Gunnoe, *ACS Catal.* **2018**, *8*, 3138–3149.
- [21] a) C. Walling, M. F. Mayahi, *J. Am. Chem. Soc.* **1959**, *81*, 1485–1489; b) J. M. Tedder, *Angew. Chem. Int. Ed.* **1982**, *21*, 401–410; *Angew. Chem.* **1982**, *94*, 433–442.
- [22] a) H. Kunkely, A. Vogler, *Z. Naturforsch.* **2013**, *68b*, 891–894; b) K. Ohkubo, K. Hirose, *Angew. Chem. Int. Ed.* **2017**, *56*, 1–5; *Angew. Chem.* **2017**, *129*, 1–1; c) A. Hu, J.-J. Guo, H. Pan, Z. Zuo, *Science* **2018**, *361*, 668–672; d) M. Zhao, W. Lu, *Org. Lett.* **2017**, *19*, 4560–4563; e) M. Zhao, W. Lu, *Org. Lett.* **2018**, *20*, 5264–5267; f) J. Xie, R. Jin, A. Li, Y. Bi, Q. Ruan, Y. Deng, Y. Zhang, S. Yao, G. Sankar, D. Ma, J. Tang, *Nature Catal.* **2018**, *1*, 889–896.
- [23] *CRC Handbook of Chemistry and Physics*, 97th ed. (Ed.: W. M. Haynes), Taylor & Francis Group, Boca Raton, FL, **2017**, pp. 88–97.
- [24] R. A. Periana, O. Mirinov, D. J. Taube, S. Gamble, *Chem. Commun.* **2002**, 2376–2377.
- [25] a) A. L. Ternay Jr., D. Deavenport, G. Bledsoe, *J. Org. Chem.* **1974**, *39*, 3268–3271; b) T. Hogan, A. Sen, *J. Am. Chem. Soc.* **1997**, *119*, 2642–2646.
- [26] a) G. M. Kramer, *Tetrahedron* **1986**, *42*, 1071–1077; b) E. S. Rudakov, L. K. Volkova, *Russ. Chem. Bull.* **2008**, *57*, 1611–1626; c) D. R. Adams, P. D. Bailey, I. D. Collier, S. A. H. Leah, C. Ridyard, *Chem. Commun.* **1996**, 333–334.
- [27] *CRC Handbook of Chemistry and Physics*, 99 ed. (Ed.: J. R. Rumble), CRC Press/Taylor & Francis, Boca Raton, FL, **2018**.
- [28] D. D. Tanner, J. E. Rowe, A. Potter, *J. Org. Chem.* **1986**, *51*, 457–460.
- [29] H. Böhme, R. Schmitz, *Chem. Ber.* **1955**, *88*, 357–361.
- [30] F. Cech, M. Linskeseder, E. Zbiral, *Monatsh. Chem.* **1976**, *107*, 1429–1436.
- [31] a) Z. J. Li, A. Pirasteh, *Int. J. Chem. Kinet.* **2006**, *38*, 386–398; b) S. M. Aschmann, R. Atkinson, *Int. J. Chem. Kinet.* **1995**, *27*, 613–622.
- [32] G. Schmitz, *Phys. Chem. Chem. Phys.* **1999**, *1*, 1909–1914.
- [33] a) Z. Li, A. Pirasteh, *Int. J. Chem. Kinet.* **2006**, *38*, 386–398; b) S. M. Aschmann, R. Atkinson, *J. Chem. Kinet.* **1995**, *27*, 613–622.
- [34] a) M. I. Christie, R. S. Roy, B. A. Thrush, *Trans. Faraday Soc.* **1959**, *55*, 1149–1152; b) W. W. Hess, E. S. Huyser, J. Kleinber, *J. Org. Chem.* **1964**, *29*, 1106–1109; c) C. C. Kelly, W. H. S. Yu, M. H. J. Wijnen, *Can. J. Chem.* **1970**, *48*, 603–606; d) C. C. Kelly, M. H. J. Wijnen, *J. Phys. Chem.* **1969**, *73*, 2447–2448.

Manuscript received: July 2, 2019

Revised manuscript received: August 7, 2019

Version of record online: September 25, 2019